## Accepted Article

**Authors:** Yiyuan Han, Zhixing Lin, Jiajing Zhou, Gyeongwon Yun, Rui Guo, Joseph J. Richardson, and Frank Caruso

WILEY-VCH

## RESEARCH ARTICLE

WILEY-VCH

# Polyphenol-Mediated Assembly of Proteins for Engineering Functional Materials

Yiyuan Han, Zhixing Lin, Jiajing Zhou, Gyeongwon Yun, Rui Guo, Joseph J. Richardson and Frank Caruso*

[*]     Y. Han, Z. Lin, Dr. J. Zhou, Dr. G. Yun, R. Guo, Dr. J. J. Richardson, Prof. F. Caruso
        ARC Centre of Excellence in Convergent Bio-Nano Science and Technology, Department of Chemical Engineering, The University of Melbourne, Parkville,
        Victoria 3010, Australia
        E-mail: fcaruso@unimelb.edu.au

        Supporting information for this article is given via a link at the end of the document.

**Abstract:** Functional materials composed of proteins have attracted much interest owing to the inherent and diverse functionality of proteins. However, establishing facile and general techniques for assembling proteins into nanomaterials is challenging owing to the complex physicochemical nature and potential denaturation of proteins. Here a simple, versatile strategy is introduced to fabricate functional protein assemblies through the interfacial assembly of proteins (>10 studied herein) and polyphenols (e.g., tannic acid) on various substrates (organic, inorganic, and biological). The dominant interactions (hydrogen bonding, hydrophobic and ionic interactions) between the proteins and tannic acid are elucidated—most proteins undergo multiple noncovalent-stabilizing interactions with polyphenols, which can be used to engineer responsiveness into the assemblies. As demonstrated, the proteins retain their structure and function within the assemblies, thereby enabling their use in various applications (e.g., catalysis, fluorescent imaging, and cell targeting).

## Introduction

Naturally occurring building blocks that can assemble into functional materials have attracted scientific interest.[1] Proteins, as biologically functional macromolecules involved in most fundamental processes of living organisms, can mediate specific interactions with diverse macromolecules for various applications including catalysis, biosensing, diagnostics, and therapy.[2] However, protein assembly is often achieved on a case-by-case basis owing to the sensitivity of proteins to denaturation and the chemical specificity of assembly routes.[3] In addition, simple and versatile strategies for assembling proteins on substrates are limited, as the noncovalent interactions between proteins and substrates are often insufficiently strong to effectively tether them to surfaces.[4] Therefore, developing versatile protein assembly strategies are important to: i) deposit proteins onto various surfaces of different sizes, aspect ratios, and material classes; ii) assemble a range of proteins; iii) preserve the structure and function of the proteins after assembly; and iv) allow for various physicochemical properties to be introduced into the assemblies.[5]
In the present study, we develop a general platform for assembling functional protein materials via a simple, versatile polyphenol-mediated coating strategy. Polyphenols (e.g., tannic acid (TA)) are ubiquitous, universally adherent natural compounds that can form conjugates with various macromolecules, particularly proteins.[6] Therefore, various proteins (more than 10 types, including enzymes, antibodies,

transport proteins, and fluorescent proteins) are assembled onto diverse substrates of different composition, size, and shape (**Figure 1**a) with different phenolics (e.g., TA, gallic acid, and epigallocatechin gallate) (Figure S1, Supporting Information). Polyphenols exhibit multiple interactions with proteins including hydrogen bonding, and hydrophobic and ionic interactions (Figure 1b).[7] These interactions allow for robust and responsive protein–polyphenol networks to be deposited, where, for instance, free-standing protein–polyphenol capsules are obtained after coating and dissolution of spherical sacrificial templates (Figure 1c).[8] Owing to the purely organic nature, these proteins-based systems can be exploited for various biomedical applications.[9] We demonstrate that their bioactive functions can be applied to enzyme catalysis, cell targeting, and tandem reactions (involving multicomponent functional materials) (Figure 1d). Moreover, these protein–polyphenol capsules enable the elucidation of the dominant interactions between the different proteins and TA, which is not possible by examining unstructured polyphenol–protein complexes in solution, because individual proteins in solution can be difficult to handle.[10] Applying this knowledge, pH-responsive capsules with different shrinking–swelling behaviors, which are dependent on the isoelectric point (pI) of the proteins, can be engineered. This work introduces i) a toolbox for protein assembly, ii) a model to study the interactions between proteins and other macromolecules, and iii) a versatile platform for diverse applications in biotechnology.[4,11]

## Results and Discussion

To demonstrate the versatility of the present method, protein–polyphenol assemblies were deposited on substrates of different composition, size, and shape (Figure 1e–h). Bovine serum albumin (BSA), a globular protein commonly found in blood plasma, was used as a model protein for protein–polyphenol assembly. Fluorescein isothiocyanate (FITC)-labeled BSA (FITC-BSA) was also used to visualize the assemblies. Simply, by depositing TA on a planar substrate (e.g., glass, polydimethylsiloxane (PDMS), or plastic on a centimeter scale) and subsequently adding FITC-BSA in one pot without washing, protein–polyphenol complexes (FITC-BSA–TA) were rapidly deposited, as visualized by a change in the color of the substrate after coating (Figure 1e). BSA–TA was also deposited on micro- and nanoparticles. As observed from the transmission electron microscopy (TEM) image in Figure 1f, the gold nanorods featured a distinct shell after coating. From the confocal laser scanning
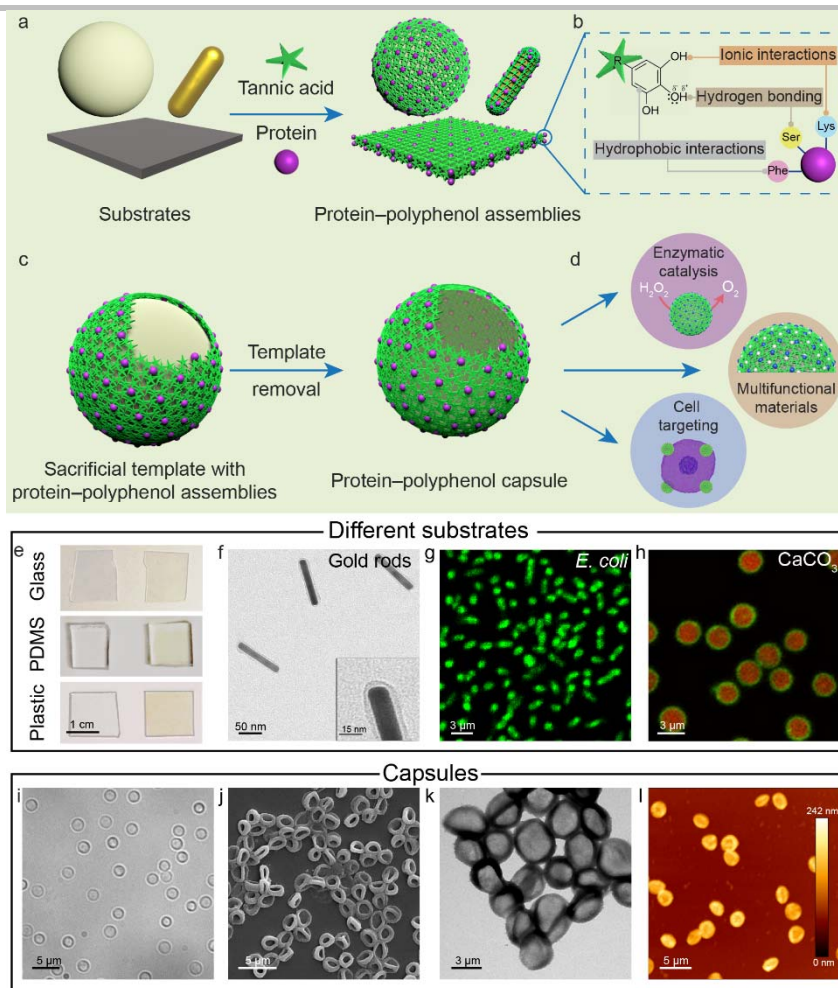
# RESEARCH ARTICLE

**Figure 1.** Interfacial protein–polyphenol assembly on various substrates. a–d) Schematic of the interfacial assembly process on different substrates (a), the different interactions between proteins and polyphenols (representative amino acids: Lys, lysine; Ser, serine; Phe, phenylalanine) (b), coating of sacrificial template and subsequent capsule formation (c), and examples of biotechnological applications of protein–polyphenol capsules (d). e) Photographs of planar substrates before (left) and after (right) coating with FITC-BSA–TA assemblies; PDMS, polydimethylsiloxane. f–h) Microscopy images of BSA–TA assemblies on various substrates: gold nanorods (TEM image) (f); *Escherichia coli* (CLSM image) (g); and TRITC-dextran-loaded CaCO$_3$ particles (h, red), FITC-BSA–TA coating shown in green. i–l) Microscopy images of BSA–TA capsules formed using sacrificial CaCO$_3$ templates: DIC (i), SEM (j), TEM (k), and AFM (l) images.

microscopy (CLSM) image in Figure 1g,h, FITC-BSA–TA coatings were observed after deposition on live *Escherichia coli* (*E. coli*) bacteria or tetramethylrhodamine (TRITC)-dextran-loaded calcium carbonate (CaCO$_3$) particles. Other organic and inorganic particles were coated with FITC-BSA–TA including polystyrene and silica (Figure S2). Collectively, these results suggest that the present protein assembly strategy is applicable to diverse substrates across multiple length scales (20 nm to 1 cm).

To study the physicochemical properties of the assemblies, CaCO$_3$ particles (3 μm in diameter) were used as sacrificial templates for preparing free-standing protein–polyphenol capsules.[12] The surface of the uncoated CaCO$_3$ particles was rough and porous. In contrast, after BSA–TA assembly, the particle surfaces were relatively smooth and appeared less porous, demonstrating that the interfacial assembly process was successful (Figure S3). Removal of the CaCO$_3$ template by ethylenediaminetetraacetic acid (EDTA) generated spherical and monodisperse BSA-TA microcapsules, as observed from the differential interference contrast (DIC) microscopy image in Figure 1i, highlighting the robust nature of the assemblies.

Compared with the BSA–TA-coated CaCO$_3$ core–shell particles (before template removal), the BSA–TA capsules demonstrated lower light scattering, indicating the successful removal of the solid CaCO$_3$ core (Figure S4a). Both the FITC-BSA–TA-coated CaCO$_3$ core–shell particles and FITC-BSA–TA capsules showed comparable fluorescence, suggesting that the template removal process did not cause significant loss of BSA (Figure S4b). Scanning electron microscopy (SEM), TEM, and atomic force microscopy (AFM) showed collapsed (air-dried) capsules, and excess polyphenol–protein aggregates, unbound or attached to the BSA–TA capsules, were not detected (Figure 1j–l). The shell thickness of the BSA–TA capsules was ~40 nm, as measured by AFM (Figure S5), and circular dichroism demonstrated that the conformation of BSA did not change after assembly[13] (Figure S6), indicating no loss of protein functionality.

A library of functional protein–polyphenol assemblies was subsequently established using TA and a variety of proteins with different pI, molecular weight ($M_w$), and aliphatic index (**Figure 2**a and Table S1),[14] which allowed for an in-depth characterization of the influence of the physicochemical properties of the proteins
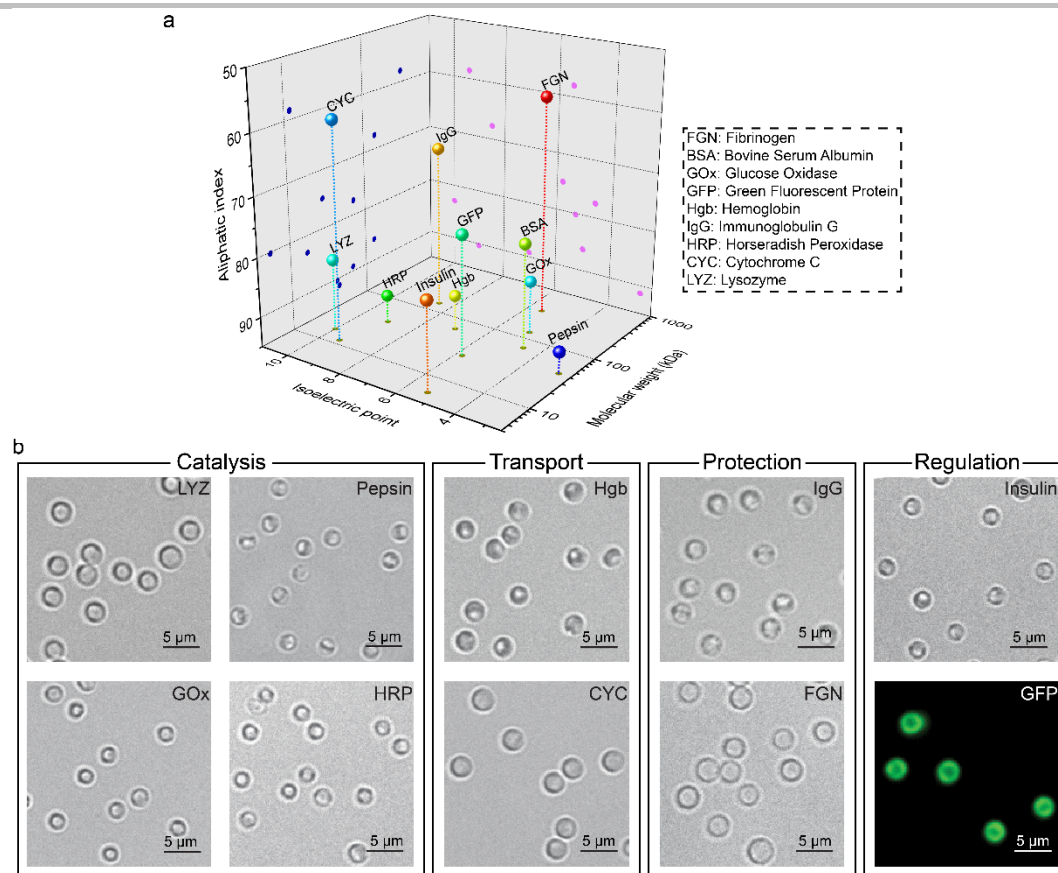
WILEY-VCH



**Figure 2.** Different protein–polyphenol capsules. a) Physicochemical properties of different proteins. (*x*-axis: isoelectric point; *y*-axis: molecular weight; and *z*-axis: aliphatic index.) b) DIC microscopy images of different protein–TA capsules and a fluorescence microscopy image of GFP–TA capsules.

on the properties of the protein–polyphenol assemblies. The functional proteins studied include lysozyme (LYZ), glucose oxidase (GOx), pepsin, horseradish peroxidase (HRP), hemoglobin (Hgb), cytochrome C (CYC), immunoglobulin G (IgG), fibrinogen (FGN), insulin, and green fluorescent protein (GFP) (Figure 2b). LYZ, GOx, HRP, and pepsin are enzymes. CYC and Hgb are essential transport proteins. IgG is a class of antibodies and FGN is responsible for blood clotting (protection proteins). Insulin is a peptide hormone and GFP is a fluorescent protein, often used as a gene expression marker (regulatory proteins). Hemeproteins (i.e., CYC and HRP) were first chosen to characterize the possible interactions between TA and the metal centers of the heme group, as polyphenols are known to chelate metals.[15] Interestingly, the mixture of hemeproteins with TA did not show the characteristic ligand-to-metal charge transfer band for polyphenol/Fe$^{III}$ complexes as observed by UV–vis spectroscopy (Figure S7), where the CYC–TA capsules featured a heme group peak at ~410 nm similarly to free CYC (Figure S8a), suggesting that TA did not competitively chelate the bound iron.[16] The Fourier transform infrared spectrum of the CYC–TA capsules demonstrated peak overlaps with the spectra of free TA and free CYC (Figure S8b). Energy-dispersive X-ray mapping results demonstrated that the CYC-TA capsules comprised four elements making up CYC and TA, namely C, N, O, and Fe (Figure S9). The loading efficiency of HRP in the HRP–TA capsules was ~80% (Figure S10 and Table S2), as determined from the iron content in HRP measured by inductively coupled plasma-optical emission spectrometry. The thicknesses of protein–TA capsules

prepared from proteins other than BSA were between 50 and 90 nm (Figure S11). Importantly, all the proteins studied herein successfully assembled at interfaces and formed conformal and robust films, likely due to the diverse interactions with TA.[17]

The structural units of proteins are amino acids, which possess different electrically charged, polar uncharged, and hydrophobic side chains. These functional side chains of amino acids can potentially interact with polyphenols via hydrogen bonding, hydrophobic interactions, and/or ionic interactions (**Figure 3**a). To investigate how these three interactions govern the stability of different protein–TA assemblies, urea, Tween 20, or sodium chloride (NaCl) was added to each of the five model protein–polyphenol capsules (LYZ–TA, IgG–TA, Hgb–TA, GOx–TA, and CYC-TA) to study disassembly over time.[6b] These proteins were chosen as model molecules, as they have different pI, $M_w$, and aliphatic index. Urea, which can participate in the formation of strong hydrogen bonds (and therefore break weaker hydrogen bonds),[18] effectively disassembled the IgG–TA and GOx–TA capsules (within 2 h), indicating that these two types of protein–polyphenol assemblies were mainly stabilized by hydrogen bonds (Figure S12a). In contrast, 90, 89, and 69% of the LYZ–TA, CYC–TA, and Hgb–TA capsules, respectively, remained after incubation with 100 mM urea for 42 h, suggesting that different or additional intermolecular forces stabilize these systems. Tween 20 is a nonionic surfactant that can form hydrophobic interactions.[19] CYC–TA, LYZ–TA, and IgG–TA capsules were completely disassembled by 100 mM Tween 20 within 5 min of incubation as a result of the hydrophobic interactions being
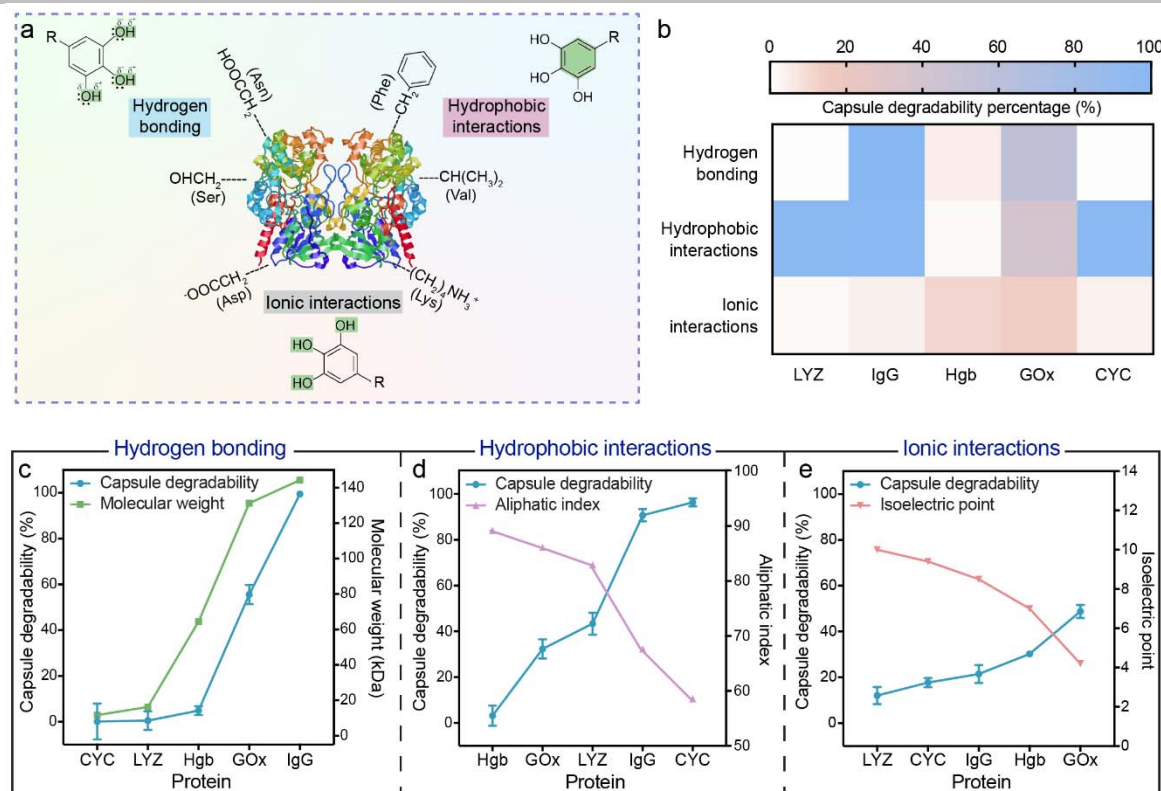
RESEARCH ARTICLE

WILEY-VCH



**Figure 3.** Dominant interactions between proteins and TA in protein–polyphenol assemblies. a) Schematic diagram of the possible interactions between the functional groups of polyphenols and proteins. Ser: serine; Asn: asparagine; Phe: phenylalanine; Val: valine; Asp: aspartic acid; Lys: lysine. b) Percentage of protein–polyphenol capsules (LYZ, IgG, Hgb, GOx, and CYC) degraded after 1 h of incubation with 100 mM of urea, Tween 20, or NaCl, highlighting the dominant interactions between the different proteins and TA. c–e) Relationship between the dominant interactions and physiochemical properties of the proteins, as analyzed from the capsule degradability of CYC–TA, LYZ–TA, Hgb–TA, GOx–TA, and IgG–TA: hydrogen bonding vs molecular weight, incubation for 1 h with 100 mM urea (c); hydrophobic interactions vs aliphatic index, incubation for 2 min with 100 mM Tween 20 (d); and ionic interactions vs isoelectric point, incubation for 19 h with 100 mM NaCl (e). Data are shown as the mean ± standard deviation (SD) ($N = 3$).

disturbed. In contrast, 50 and 75% of the GOx–TA and Hgb–TA capsules remained intact in Tween 20 solution over 40 h of incubation (Figure S12b). Incubation of the capsules in 100 mM NaCl resulted in the disassembly of all five protein–polyphenol capsules to varying extent over 90 h owing to ionic shielding— among the capsules studied, GOx–TA capsules showed the highest disassembly rate or the lowest percentage of capsules remaining (37%) after 90 h (Figure S12c). Generally, the type of protein determines which interactions are present in the assemblies (Figure 3b and Figure S13). For instance, hydrophobic interactions are the dominant stabilizers for LYZ–TA and CYC–TA, whereas they are the least dominant interactions between Hgb and TA. In IgG–TA, the most dominant interactions are hydrogen bonding and hydrophobic interactions. In GOx–TA, the interactions are governed by all three types of interactions.

To gain a deeper insight into the nature of the protein–polyphenol interactions in the assemblies, we further analyzed the relationship between the dominant interactions and the physiochemical properties of the proteins such as the size ($M_w$), aliphatic index, and pI. The three key findings are as follows. i) The strength of hydrogen bonding between polyphenols and proteins is likely based on the $M_w$ or size of the proteins as the peptide backbone and the majority of the exposed protein surface (polar amino acids) are hydrophilic. For example, the molecular size of the proteins increases in the order of CYC < LYZ < Hgb < GOx < IgG, and the disassembly rate of the respective protein–

TA capsules also increases in the same order as hydrogen bonds between the proteins and hydroxyl groups of the catechol/gallol moieties in polyphenols are disrupted (Figure 3c). ii) Proteins with high aliphatic indexes containing more aliphatic and hydrophobic side chains (such as alanine, valine, isoleucine, and leucine) can form stronger hydrophobic interactions with the aromatic groups of polyphenols compared with proteins with low aliphatic indexes (low hydrophobicity). For example, the interactions of polyphenols with high aliphatic index proteins, such as Hgb and GOx, are more difficult to disrupt using surfactants when compared with those of polyphenols with low aliphatic index proteins such as CYC and IgG (Figure 3d). iii) The strength of ionic interactions between proteins and polyphenols depends on the charge of the protein. For instance, the pI of the proteins increases in the order of GOx < Hgb < IgG < CYC < LYZ, which correlates to the relatively more positively charged side chains in the protein and thereby enhanced ionic interactions with the deprotonated hydroxyls of the catechol/gallol moieties of polyphenols (Figure 3e). These results highlight the complex nature in which polyphenols interact with different proteins at the molecular level, suggesting that TA is essential for helping to construct amino acid-based materials.

The protein–polyphenol assemblies exhibited distinct and tunable pH-responsive properties, owing to the various p$K_a$ values of the hydroxyl groups of TA and the pIs of the different proteins. For example, BSA–TA capsules swelled from 2.1 to 4.2 μm when the environmental pH increased from 4.0 to 7.4 and shrank to their
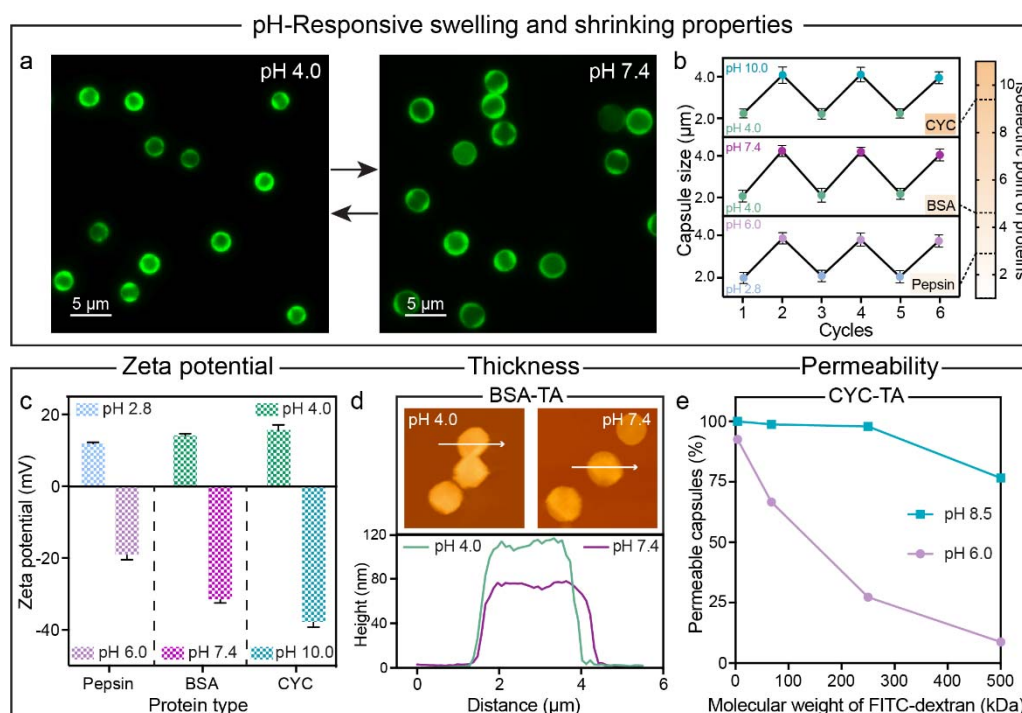
# RESEARCH ARTICLE

WILEY-VCH



**Figure 4.** pH-Responsiveness of protein–polyphenol assemblies. a) Fluorescence microscopy images of the BSA–TA capsules at pH 4.0 and pH 7.4. b) Changes in the diameters of the pepsin–TA, BSA–TA, and CYC–TA capsules as a function of pH wash cycle. The diameters of 20 capsules were measured using DIC microscopy, and data are shown as the mean ± SD. c) Zeta potential values of the pepsin–TA, BSA–TA, and CYC–TA capsules at different pH. Data are shown as the mean ± SD. d) AFM images and corresponding height measurements of the BSA–TA capsules at pHs 4.0 and 7.4. e) Percentage of permeable capsules plotted against FITC-dextran of different molecular weight at pHs 8.5 and 6.0. The permeability of 100 capsules was measured using CLSM.

original size when the pH was lowered to 4.0 (**Figure 4**a). This swelling/shrinking process could be repeated reproducibly over multiple cycles (Figure 4b). TA and BSA both possess a net negative charge when the pH rises above the pI of BSA (4.6), which leads to electrostatic repulsion, and thus swelling, and eventual dissociation. The other protein–TA capsules also showed reversible pH-responsive swelling and shrinking behaviors when the pI values of the proteins (pepsin: 2.9; CYC: 9.6) were within the swelling/shrinking values (pepsin: pH 2.8–6.0 and CYC: pH 4.0–10.0), which supports our proposed mechanism (Figure 4b and Figure S14). In addition, the zeta potential of the pepsin–TA, BSA–TA, and CYC–TA capsules changed under different pH, further suggesting the importance of the protonation state of the proteins (Figure 4c). The thickness of the BSA–TA capsules decreased from ~50 nm at pH 4.0 to ~30 nm at pH 7.4, which demonstrates that the swelling behavior stretches the films to accommodate for the increase in volume of the capsule (Figure 4d and Figure S15). As such pH-responsiveness can be desirable for drug delivery applications, the molecular permeability of the CYC–TA capsules was assessed using FITC-dextran of different molecular weights as the model cargo. As observed in Figure 4e, the permeability of the CYC–TA capsules was pH dependent, suggesting that these assemblies could be used to load and release drugs under specific pH environments. For instance, ~25% of the CYC–TA capsules were permeable to 250 kDa FITC-dextran at pH 6.0, whereas nearly 100% of the capsules were permeable at pH 8.5 (Figure 4f and Figure S16), which corresponds to higher permeability when the capsules are swollen. When considering physiological pH changes, such as the stomach (pH 1.0–3.0), blood (pH 7.4), or duodenum (pH 4.8–

8.2),[20] we envision that our polyphenol–protein assemblies could serve as smart delivery systems for various biomedical applications.

The potential biotechnological applications of the protein–polyphenol assemblies were examined. The functionality of the protein–polyphenol assemblies for catalysis was first investigated. HRP is a common enzyme that catalyzes the oxidation of various organic substrates in the presence of $H_2O_2$.[21] Specifically, the conversion of amplex red (AR) into resorufin (RS), which has a strong absorbance at 560 nm,[22] in the presence of the HRP–TA assemblies (core–shell particles and capsules) was examined (**Figure 5**a). The HRP–TA capsules showed comparable catalytic activity to free HRP, suggesting that the enzymatic activity was not affected after assembly (Figure 5b and Figure S17).[23] Moreover, these capsules showed higher catalytic activity (~25%) than the HRP–TA core–shell particles, which is attributed to the likely improved mass transfer in the hollow (capsule) system. In addition, the enzymes in the HRP–TA capsules displayed excellent recyclability, where more than 68% of the initial HRP activity was retained after five cycles of catalysis and collection (Figure 5c).

Multicomponent systems composed of GOx and HRP (GOx&HRP–TA) were engineered and investigated to conduct a cascade reaction.[24] Specifically, GOx can catalyze the oxidation and hydrolysis of β-D-glucose into gluconic acid and $H_2O_2$, and HRP can catalyze AR oxidation to RS in the presence of the generated $H_2O_2$ (Figure 5d). The GOx&HRP–TA capsules showed successful colorimetric reaction with glucose in contrast to the (single-component) GOx–TA and HRP–TA capsules (Figure 5e). Therefore, the current approach adopted to prepare
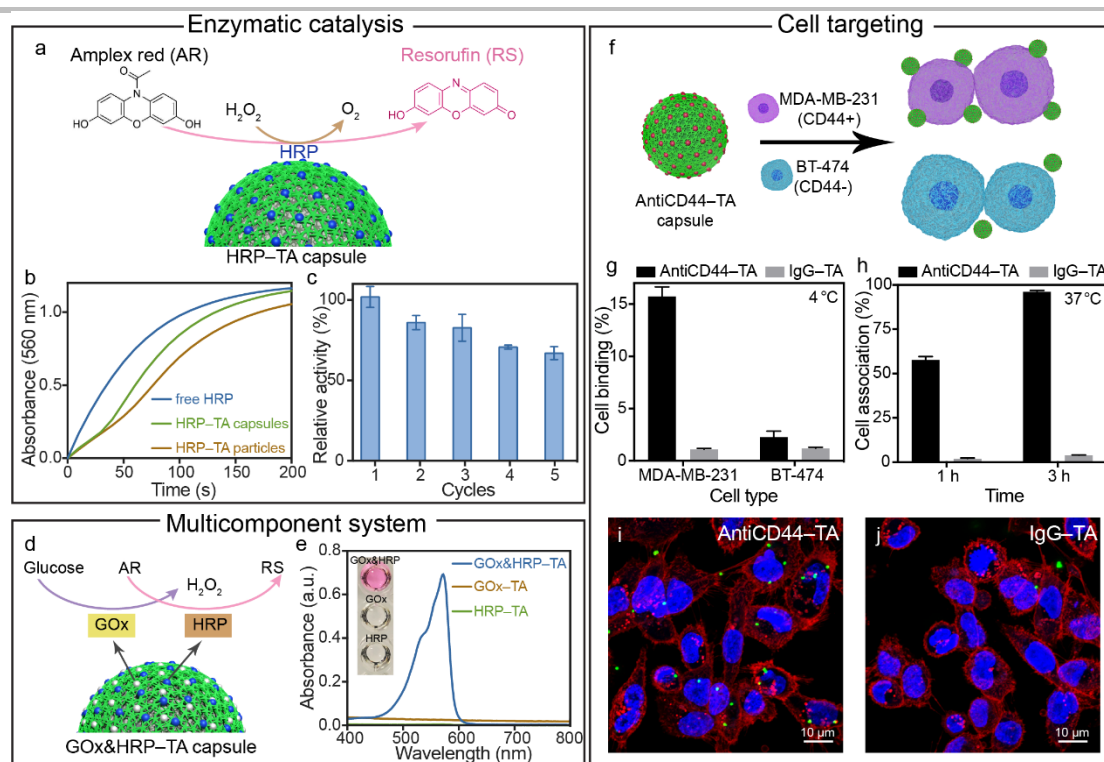
**Figure 5.** Protein–polyphenol assemblies for diverse applications. a–c) Enzymatic activity of the HRP–TA capsules. Schematic of the HPR-catalyzed oxidation of AR to RS over the HRP–TA capsules (a). Time-dependent absorbance changes as a result of the oxidation of AR by different catalytic systems: free HRP, HRP–TA capsules, and HRP–TA core–shell particles (b). Changes in the relative catalytic activity of the HRP–TA capsules as a function of cycle number (c). d–e) Cascade reaction using multicomponent GOx&HRP–TA capsules: schematic of glucose-triggered AR oxidation to produce RS in the presence of GOx and HRP (d) and UV–vis spectra of the cascade reaction using different single- and multicomponent capsule systems (e). Inset: color changes using the different systems. f–j) Cell targeting of antibody–TA capsules: schematic of the targeting specificity of antiCD44–TA capsules toward CD44 overexpressing (CD44+) cells (MDA-MB-231 cells) and CD44 minimal expressing (CD44−) cells (BT-474 cells) (f); flow cytometry analysis of the antiCD44–TA and IgG–TA capsules binding to MDA-MB-231 and BT-474 cells after incubation for 1 h at 4 °C (g); percentage of MDA-MB-231 cells associated with antiCD44–TA and IgG–TA capsules after 1 or 3 h incubation at 37 °C (h); and CLSM images of antiCD44–TA (i) and IgG–TA capsules (j) incubated with MDA-MB-231 cells for 3 h at 37 °C. The capsule-to-cell ratio was 50:1 in all cell experiments. Data are shown as the mean ± SD ($N$ = 3).

the multicomponent and multifunctional protein–polyphenol assemblies presents a simple and versatile strategy to design intricate biomimetic systems.[25]

Proteins also plays a significant role in recognition, such as cell targeting by antibodies.[26] Antibody–TA capsules were thus synthesized to study their cell binding and targeting ability. CD44, a cell-surface glycoprotein involved in cell–cell interactions, is overexpressed on many types of cancer cell membranes,[27] and anti-CD44 antibodies can specifically target CD44 overexpressing (CD44+) cells, but do not readily interact with CD44 minimal expressing (CD44−) cells (Figure 5f). The cell binding and targeting ability of antiCD44–TA capsules were investigated using two human breast cancer cell lines, MDA-MB-231 (CD44+) cells and BT-474 (CD44−) cells; IgG–TA (anti-Human IgG) capsules were used as the negative control. Cell binding was performed at 4 °C after 1 h incubation to prevent internalization.[28] The antiCD44–TA capsules showed high binding specificity toward CD44+ cells over CD44− cells, whereas the IgG–TA capsules demonstrated nonspecific cell binding toward both cells (Figure 5g and Figure S18). In addition, cell association experiments with CD44+ cells were performed at 37 °C after 1 and 3 h incubation to compare the antiCD44–TA capsules with control IgG–TA capsules. The flow cytometry results showed that after 1 h incubation, 58% of the MDA-MB-231 (CD44+) cells associated with the antiCD44–TA capsules, whereas only 2% of the MDA-MB-231 cells associated with the IgG–TA capsules (Figure 5h). After 3 h, the difference in cell association became more

significant—96% of the MDA-MB-231 cells associated with the antiCD44–TA capsules, whereas only 4% of the MDA-MB-231 cells associated with the IgG–TA capsules (Figure 5h and Figure S18), as supported visually by CLSM (Figure 5i,j). These above results reveal that the formation of antibody–TA assemblies does not negatively affect the inherent targeting ability of the antibodies. Additionally, the BSA–TA and LYZ–TA capsules displayed excellent stability in serum (Figure S19), negligible cytotoxicity and were internalized in cells (~100% capsules internalized by cells after 14 h, Figure S20), highlighting that this assembly strategy shows potential for intracellular protein delivery applications.[29] Moreover, protein–TA capsules did not have significant interactions with live *E. coli*, indicating that these coatings have the potential to endow materials with low-fouling properties (Figure S21).[30] To improve reproducibility, reporting, and re-analysis, this study conforms to the Minimum Information Reporting in Bio–Nano Experimental Literature (MIRIBEL) standard,[31] and a companion checklist is provided in the Supporting Information.

## Conclusion

We have introduced interfacial polyphenol-mediated protein assembly as a versatile and strategy to create a library of functional protein-based materials. Protein–polyphenol

# RESEARCH ARTICLE

assemblies can be deposited on various substrates of different composition, size, and shape, affording new possibilities for surface modification. This technique is applicable to a wide range of proteins of diverse physicochemical properties and biological functions, thus enabling bioactive surface coating and functional capsule formation. Moreover, the protein–polyphenol capsules can be used to elucidate the dominant interaction(s) between different proteins and polyphenols; the results reveal that the molecular weight (size), hydrophobicity (aliphatic index), and isoelectric point (electrical charge) of the protein determine the strength of hydrogen bonding, hydrophobic interactions, and ionic interactions, respectively. These various noncovalent-stabilizing interactions between proteins and polyphenols offer possibilities to engineer assemblies with desirable responsiveness to multiple stimuli such as changes in pH, as exemplified. Finally, we have demonstrated various applications for the protein–polyphenol assemblies, as a range of functionalities can be engineered into the assemblies through judicious choice of the constituent proteins. This platform is expected to advance both fundamental and applied research owing to its simplicity and versatility.

## Acknowledgements

## Competing interests

The authors declare no competing interests.

**Keywords:** biocatalysis • cancer target • particle surface engineering • polyphenols • proteins

[1]     a) H. Ejima, J. J. Richardson, K. Liang, J. P. Best, M. P. van Koeverden, G. K. Such, J. Cui, F. Caruso, *Science* **2013**, *341*, 154-157; b) J. Guo, B. L. Tardy, A. J. Christofferson, Y. Dai, J. J. Richardson, W. Zhu, M. Hu, Y. Ju, J. Cui, R. R. Dagastine, I. Yarovsky, F. Caruso, *Nat. Nanotechnol.* **2016**, *11*, 1105-1111.

[2]     a) J. A. Shadish, G. M. Benuska, C. A. DeForest, *Nat. Mater*. **2019**, *18*, 1005-1014; b) C. D. Spicer, C. Jumeaux, B. Gupta, M. M. Stevens, *Chem. Soc. Rev*. **2018**, *47*, 3574-3620.

[3]     a) X. Huang, M. Li, D. C. Green, D. S. Williams, A. J. Patil, S. Mann, *Nat. Commun.* **2013**, *4*, 2239; b) Q. Luo, C. Hou, Y. Bai, R. Wang, J. Liu, *Chem. Rev.* **2016**, *116*, 13571-13632; c) T. P. Knowles, T. W. Oppenheim, A. K. Buell, D. Y. Chirgadze, M. E. Welland, *Nat. Nanotechnol.* **2010**, *5*, 204-207.

[4]     R. Liu, J. Zhao, Q. Han, X. Hu, D. Wang, X. Zhang, P. Yang, *Adv. Mater.* **2018**, *30*, 1802851.

[5]     E. V. Skorb, D. V. Andreeva, *Adv. Funct. Mater.* **2013**, *23*, 4483-4506.

[6]     a) M. A. Rahim, S. L. Kristufek, S. Pan, J. J. Richardson, F. Caruso, *Angew. Chem.* **2019**, *131*, 1920-1945; *Angew. Chem. Int. Ed.* **2019**, *58*, 1904-1927; b) J. E. Chung, S. Tan, S. J. Gao, N. Yongvongsoontorn, S. H. Kim, J. H. Lee, H. S. Choi, H. Yano, L. Zhuo, M. Kurisawa, J. Y. Ying, *Nat. Nanotechnol.* **2014**, *9*, 907-912.

[7]     S. Quideau, D. Deffieux, C. Douat-Casassus, L. Pouysegu, *Angew. Chem.* **2011**, *123*, 610-646; *Angew. Chem. Int. Ed.* **2011**, *50*, 586-621.

[8]     F. Caruso, R. A. Caruso, H. Möhwald, *Science* **1998**, *282*, 1111-1114.

[9]     a) U. Shimanovich, G. J. Bernardes, T. P. Knowles, A. Cavaco-Paulo, *Chem. Soc. Rev.* **2014**, *43*, 1361-1371; b) M. Yan, J. Du, Z. Gu, M. Liang, Y. Hu, W. Zhang, S. Priceman, L. Wu, Z. H. Zhou, Z. Liu, *Nat. Nanotechnol.* **2010**, *5*, 48-53.

[10]     a) P. Bandyopadhyay, A. K. Ghosh, C. Ghosh, *Food Funct.* **2012**, *3*, 592-605; b) A. Papadopoulou, R. J. Green, R. A. Frazier, *J. Agric. Food Chem.* **2005**, *53*, 158-163.

[11]     a) M. Shin, H.-A. Lee, M. Lee, Y. Shin, J.-J. Song, S.-W. Kang, D.-H. Nam, E. J. Jeon, M. Cho, M. Do, S. Park, M. S. Lee, J.-H. Jang, S.-W. Cho, K.-S. Kim, H. Lee, *Nat. Biomed. Eng.* **2018**, *2*, 304-317; b) C. Liu, T. Wan, H. Wang, S. Zhang, Y. Ping, Y. Cheng, *Sci. Adv.* **2019**, *5*, eaaw8922.

[12]     J. J. Richardson, J. W. Maina, H. Ejima, M. Hu, J. Guo, M. Y. Choy, S. T. Gunawan, L. Lybaert, C. E. Hagemeyer, B. G. De Geest, *Adv. Sci.* **2015**, *2*, 1400007.

[13]     a) N. J. Greenfield, G. D. Fasman, *Biochemistry* **1969**, *8*, 4108-4116; b) N. J. Greenfield, *Nat. Protoc.* **2006**, *1*, 2876-2890.

[14]     P. G. Righetti, G. Tudor, K. Ek, *J. Chromatogr. A* **1981**, *220*, 115-194.

[15]     J. Guo, Y. Ping, H. Ejima, K. Alt, M. Meissner, J. J. Richardson, Y. Yan, K. Peter, D. von Elverfeldt, C. E. Hagemeyer, F. Caruso, *Angew. Chem.* **2014**, *126*, 5652-5657; *Angew. Chem. Int. Ed.* **2014**, *53*, 5546-5551.

[16]     M. A. Rahim, K. Kempe, M. Müllner, H. Ejima, Y. Ju, M. P. van Koeverden, T. Suma, J. A. Braunger, M. G. Leeming, B. F. Abrahams, F. Caruso, *Chem. Mater.* **2015**, *27*, 5825–5832.

[17]     K. J. Siebert, N. V. Troukhanova, P. Y. Lynn, *J. Agric. Food Chem.* **1996**, *44*, 80-85.

[18]     L. B. Sagle, Y. Zhang, V. A. Litosh, X. Chen, Y. Cho, P. S. Cremer, *J. Am. Chem. Soc.* **2009**, *131*, 9304-9310.

[19]     N. B. Bam, J. L. Cleland, T. W. Randolph, *Biotechnol. Prog.* **1996**, *12*, 801-809.

[20]     D. Schmaljohann, *Adv. Drug Delivery Rev.* **2006**, *58*, 1655-1670.

[21]     N. C. Veitch, *Phytochemistry* **2004**, *65*, 249-259.

[22]     M. Zhou, Z. Diwu, N. Panchuk-Voloshina, R. P. Haugland, *Anal. Biochem.* **1997**, *253*, 162-168.

[23]     a) H. Tan, S. Guo, N. D. Dinh, R. Luo, L. Jin, C. H. Chen, *Nat. Commun.* **2017**, *8*, 663; b) K. Li, G. Xiao, J. J. Richardson, B. L. Tardy, H. Ejima, W. Huang, J. Guo, X. Liao, B. Shi, *Adv. Sci.* **2019**, *6*, 1801688.

[24]     I. Wheeldon, S. D. Minteer, S. Banta, S. C. Barton, P. Atanassov, M. Sigman, *Nat. Chem.* **2016**, *8*, 299-309.

[25]     a) N. P. King, J. B. Bale, W. Sheffler, D. E. McNamara, S. Gonen, T. Gonen, T. O. Yeates, D. Baker, *Nature* **2014**, *510*, 103-108; b) B. O. Okesola, A. Mata, *Chem. Soc. Rev.* **2018**, *47*, 3721-3736.

[26]     a) A. M. Scott, J. D. Wolchok, L. J. Old, *Nat. Rev. Cancer* **2012**, *12*, 278-287; b) L. M. Weiner, R. Surana, S. Wang, *Nat. Rev. Immunol.* **2010**, *10*, 317-327.

[27]     H. Ponta, L. Sherman, P. A. Herrlich, *Nat. Rev. Mol. Cell Biol.* **2003**, *4*, 33-45.

[28]     A. Lesniak, A. Salvati, M. J. Santos-Martinez, M. W. Radomski, K. A. Dawson, C. Åberg, *J. Am. Chem. Soc.* **2013**, *135*, 1438-1444.

[29]     a) M. P. Stewart, A. Sharei, X. Ding, G. Sahay, R. Langer, K. F. Jensen, *Nature* **2016**, *538*, 183-192; b) F. Scaletti, J. Hardie, Y. W. Lee, D. C. Luther, M. Ray, V. M. Rotello, *Chem. Soc. Rev.* **2018**, *47*, 3421-3432.

[30]     W. Luo, G. Xiao, F. Tian, J. J. Richardson, Y. Wang, J. Zhou, J. Guo, X. Liao, B. Shi, *Energy Environ. Sci.* **2019**, *12*, 607–614.

[31]     M. Faria, M. Björnmalm, K. J. Thurecht, S. J. Kent, R. G. Parton, M. Kavallaris, A. P. Johnston, J. J. Gooding, S. R. Corrie, B. J. Boyd, P. Thordarson, A. K. Whittaker, M. M. Stevens, C. A. Prestidge, C. J. H. Porter, W. J. Parak, T. P. Davis, E. J. Crampin, F. Caruso, *Nat. Nanotechnol.* **2018**, *13*, 777-785.

WILEY-VCH

## Entry for the Table of Contents
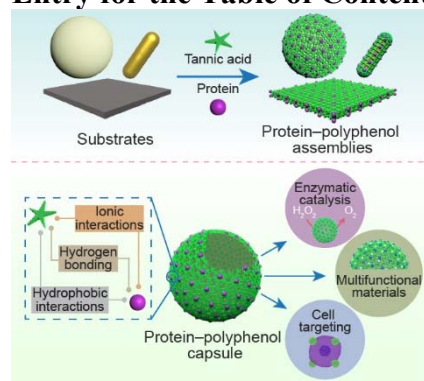


A simple and versatile strategy for assembling functional nanomaterials is established through the interfacial assembly of proteins and polyphenols on various substrates. Protein–polyphenol capsules are used to elucidate the dominant interaction(s) between different proteins and polyphenols. The assembled proteins retain their structure and function, thereby enabling their use in various applications (e.g. biocatalysis or cell targeting).